Self-assembling peptide hydrogel fosters chondrocyte extracellular matrix production and cell division: Implications for cartilage tissue repair

J. Kisiday*, M. Jin†, B. Kurz‡, H. Hung‡, C. Semino§, S. Zhang§¶, and A. J. Grodzinsky*†‡§¶

*Biological Engineering Division, Departments of †Mechanical and ‡Electrical Engineering, §Center for Biomedical Engineering, Massachusetts Institute of Technology, Cambridge, MA 02139-4307

Communicated by John M. Buchanan, Massachusetts Institute of Technology, Cambridge, MA, May 23, 2002 (received for review February 23, 2002)

Emerging medical technologies for effective and lasting repair of articular cartilage include delivery of cells or cell-seeded scaffolds to a defect site to initiate *de novo* tissue regeneration. Biocompatible scaffolds assist in providing a template for cell distribution and extracellular matrix (ECM) accumulation in a three-dimensional geometry. A major challenge in choosing an appropriate scaffold for cartilage repair is the identification of a material that can simultaneously stimulate high rates of cell division and high rates of cell synthesis of phenotypically specific ECM macromolecules until repair evolves into steady-state tissue maintenance. We have devised a self-assembling peptide hydrogel scaffold for cartilage repair and developed a method to encapsulate chondrocytes within the peptide hydrogel. During 4 weeks of culture *in vitro*, chondrocytes seeded within the peptide hydrogel retained their morphology and developed a cartilage-like ECM rich in proteoglycans and type II collagen, indicative of a stable chondrocyte phenotype. Time-dependent accumulation of this ECM was paralleled by increases in material stiffness, indicative of deposition of mechanically functional neo-tissue. Taken together, these results demonstrate the potential of a self-assembling peptide hydrogel as a scaffold for the synthesis and accumulation of a true cartilage-like ECM within a three-dimensional cell culture for cartilage tissue repair.

three-dimensional cell culture | biological scaffold | regenerative medicine

Articular cartilage defects, resulting from traumatic injury or degenerative diseases, may require novel regenerative medicine strategies for restoration of biologically and mechanically functional tissue. One approach relies on delivering cells within voids created by the removal of dysfunctional or damaged tissue (1). Implanted cells within the wound bed may initiate a repair response through *de novo* cellular regulation. This strategy remains a significant challenge in current healthcare technologies. Delivery of chondrocytes to a cartilage defect may be facilitated by attachment to or encapsulation within a scaffold. Tissue engineering scaffolds must be completely biocompatible, without the potential to degrade into harmful residues. The scaffold defines a three-dimensional (3D) template in which chondrocytes produce and deposit extracellular matrix (ECM). Structural stability of the cell/scaffold system must be maintained by the scaffold until seeded chondrocytes have deposited a continuous network of ECM throughout the implant. Ideally, the scaffold would then degrade as the ECM network matures, guiding regeneration throughout the entire scaffold geometry. A successful cartilage replacement must integrate with surrounding normal cartilage, and the newly assembled ECM must provide tissue resilience to tissue compression that occurs during normal joint loading.

A variety of biologically derived and synthetic polymeric and hydrogel materials are actively under investigation as scaffolds for cartilage tissue repair (2). Collagen-based scaffolds [e.g., type I collagen gel (3) and type I and type II collagen sponges (4, 5)], polyglycolic acid and polylactic acid (6), fibrin (7), alginate (8), and polyethlene oxide (9) have been studied *in vitro* to characterize chondrocyte division and phenotypic expression as well as ECM production. Animal studies have also been conducted with these scaffolds, as well as a hyaluronon derivative, to test ECM formation and cell-scaffold integration *in vivo* (6, 10–14). Whereas many scaffolds maintain differentiated chondrocytes and accumulate ECM matrix *in vitro* and/or in animals, no clinical application of a scaffold-based cartilage repair tissue is yet available.

A new class of peptide-based biomaterials has been actively pursued as a molecular-engineered scaffold for tissue repair. Certain peptides are able to self-assemble into stable hydrogels at low (0.1–1%) peptide concentrations (15–17). Such self-assembling peptides are characterized by amino acid sequences of alternating hydrophobic and hydrophilic side groups. Sequences of charged amino acid residues include alternating positive and negative charges (15–17). Self-assembling peptides form stable β-sheet structures when dissolved in deionized water. Exposure to electrolyte solution initiates β-sheet assembly into interweaving nanofibers (15–17). Such self-assembly occurs rapidly when the ionic strength of the peptide solution exceeds a certain threshold, or the pH is such that the net charge of the peptide molecules is near zero (18). Intermediate steps of self-assembly have been investigated by observing relatively slow nanofiber formation and subsequent network assembly in deionized water, without triggering rapid self-assembly by the addition of electrolytes (19). The self-assembling peptide hydrogel contains unique features for a tissue engineering polymer scaffold. The nanofiber structure is almost 3 orders of magnitude smaller than most polymer microfibers and presents a unique polymer structure with which cells may interact. In addition, peptide sequences may be designed for specific cell-matrix interactions that influence cell differentiation and tissue formation (20). Also, the synthetic nature of the peptide minimizes the risk of carrying biological pathogens relative to animal-derived biomaterials (20).

Diverse mammalian cell types have been found to attach and proliferate on the preassembled peptide gel surfaces (16). Additionally, two peptides have been tested for immunogenicity in rats. Injection of $(EAKA)_4$ and $(RADA)_4$ into leg muscle of Fisher 344 rats resulted in no detectable toxic reaction after 9 days and 5 weeks, respectively (17).

Here, we report the study of a self-assembling peptide KLD-12 hydrogel as a 3D scaffold for encapsulation of chondrocytes. Previously, investigators found that chondrocytes could maintain their phenotype or redifferentiate after serial passaging in hydrogels such as agarose (21) and alginate (22). Such model hydrogel culture systems have been useful for studying the basic biology of chondrocyte biosynthesis of ECM (23) and cellular response to mechanical loading (24) *in vitro*. In this study, we hypothesized that a self-assembling peptide hydrogel would provide an appropriate environment for the retention of chondrocyte phenotype and the synthesis of a mechanically functional cartilage ECM. In addition,

Abbreviations: ECM, extracellular matrix; 3D, three-dimensional; ITS, insulin, transferrin, and selenium; GAG, glycosaminoglycan; MTS, 3-(4,5-dimethylthiazol-2-yl)-5-(3-carboxymethoxyphenyl)-2-(4-sulfophenyl)-2H-tetrazolium.

¶To whom reprint requests may be addressed. E-mail: alg@mit.edu or shuguang@mit.edu.

 www.pnas.org/cgi/doi/10.1073/pnas.142309999

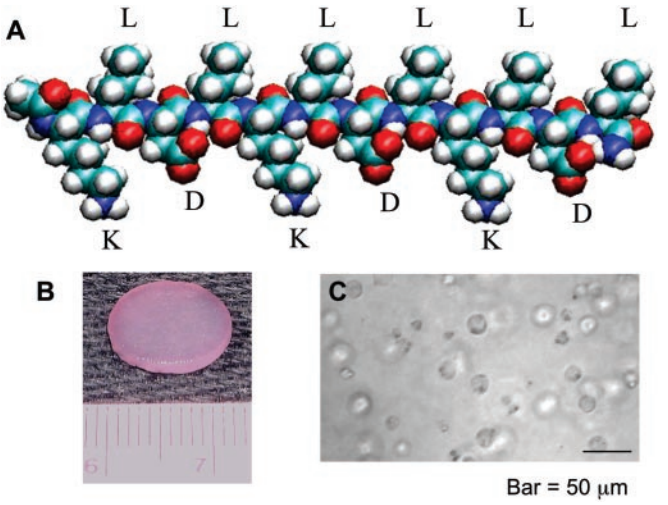

Fig. 1. (*A*) Molecular model of a single KLD-12 self-assembling peptide. The alternating hydrophobic and hydrophilic residues on the backbone promote β-sheet formation. The positively charged lysines (K) and negatively charged aspartic acids (D) are on the lower side of the β-sheet, and the hydrophobic leucines (L) are on the upper side. This molecular structure facilitates self-assembly through intermolecular interactions. (*B*) A 12-mm chondrocyte-seeded peptide hydrogel plug, punched from 1.6-mm-thick slabs. (*C*) Light microscope image of chondrocytes encapsulated in peptide hydrogel.

the self-assembling nature of the peptide hydrogel and the flexibility of molecular design may offer advantages in controlling scaffold degradation, cell attachment, and the delivery of tethered stimulatory growth factors to the microenvironment of encapsulated cells. Together, these features offer a flexible approach to optimizing scaffold-cell interactions for cartilage repair.

Materials and Methods

Isolation of Chondrocytes and Casting of Cell-Seeded Peptide and Agarose Hydrogels. Chondrocytes were isolated from the femoropatellar grooves of 1- to 2-week-old bovine calves within several hours after slaughter, as described (25). The peptide KLD-12 with sequence AcN-KLDLKLDLKLDL-CNH_2 (Fig. 1*A*) was synthesized by using a peptide synthesizer (Applied Biosystems Peptide synthesizer 431A) and lyophilized to a powder. KLD12 powder was dissolved in 295 mM sucrose solution at a peptide concentration of 0.56% (wt/vol). Isolated chondrocytes were resuspended in a volume of sucrose solution equal to 10% of the final peptide/cell suspension volume. Peptide solution was added to obtain a final peptide concentration of 0.5% and a cell density of 15×10^6 cells per ml, with the sucrose used to maintain physiologic osmotic pressure. The suspension was lightly vortexed and injected into a stainless steel casting frame consisting of a $40 \times 40 \times 1.6$-mm window, supported on both faces by filter paper and porous mesh similar to Ragan *et al.* (25). The casting frame was placed in a 1× PBS bath to initiate self-assembly of the peptide gel into a slab structure. After 25 min, the 1.6-mm-thick seeded peptide gel was transferred to a Petri dish for long-term culture.

Chondrocyte-seeded agarose gel slabs were cast in a similar manner. Centrifuged cells were resuspended in feed medium and mixed with 3% low melting temperature agarose (SeaPlaque agarose, FMC) to obtain a final agarose concentration of 2% and a cell density of 15×10^6 cells per ml. The casting frame was placed in a room temperature 1× PBS bath to initiate gelation. After 5 min the gel slab was transferred to a Petri dish containing 4°C medium and subsequently placed in a 37° incubator. Peptide and agarose gels were cultured in 10% FBS-supplemented feed medium. Additional gel preparations were maintained in feed medium supplemented with 1% ITS (insulin, transferrin, and selenium, Sigma) plus 0.2% FBS (ITS/FBS medium). The slabs were seeded at a cell density of 15×10^6 or 30×10^6 cells per ml. Each slab was fed 12 ml of medium every other day.

Cellular Biosynthesis of ECM Macromolecules. On days 5, 10, 15, 21, and 28 of culture, groups of six 3-mm diameter by 1.6-mm thick plugs were punched from cell-seeded peptide and agarose gel slabs by using a stainless steel dermal punch. Each group of plugs was transferred to a single well of a 12-well dish containing 2 ml feed medium plus 5 μCi/ml ^{35}S-sulfate and 10 μCi/ml ^{3}H-proline. Incorporation of ^{35}S-sulfate and ^{3}H-proline are measures of the rate of synthesis of sulfated proteoglycans and total protein, respectively (26). After 20 h the plugs were removed from radiolabel medium and washed five times over 90 min in standard PBS plus 1 mM unlabeled proline and sulfate. Each cell-seeded plug was then transferred to 1-ml proteinase K (Roche Applied Science)–Tris·HCl solution and digested overnight at 60°C. From the digests, radiolabel incorporation and total accumulated sulfated glycosaminoglycan (GAG) content via DMMB dye binding were measured as described (27).

Separate control studies on day 35 of culture were performed to assess (*i*) the fraction of the radioactivity within the peptide hydrogel plugs that was in macromolecular versus low molecular weight form, (*ii*) the fraction of total newly synthesized ECM macromolecules that was retained within the peptide hydrogel versus that released to medium, and (*iii*) the fraction of ^{3}H radiolabel incorporated as hydroxyproline as a measure of newly synthesized collagen. For macromolecular analysis, radiolabeled species obtained from peptide gel extracts and medium fractions were separated into macromolecular and low molecular weight components on a PD10 gel filtration column of Sephadex G-25 (molecular weight cutoff of 1–5,000; Amersham Pharmacia) in 0.5-ml portions of elution buffer containing 1% SDS, 10 mM DTT, 50 mM Tris·HCl, pH 8.5 (21). Macromolecular components released to medium were ≈2% and ≈11% of total peptide hydrogel-accumulated ^{35}S-sulfate and ^{3}H-proline, respectively. Proteinase K-digested peptide gel plugs contained 95% macromolecular ^{35}S-sulfate. Hydrogel-accumulated ^{3}H-proline was analyzed after SDS extraction. Cell-seeded peptide hydrogel was incubated in 2% SDS, 10 mM DTT, 50 mM Tris·HCl, pH 8.5 at 100°C for 15 min. Extracted ^{3}H-proline molecules were 89% macromolecular. These data showed that the hydrogel scaffold retained ≈93% and 78% of newly synthesized proteoglycan and protein macromolecules, respectively, similar to that observed in native cartilage organ culture (27). Because of the high retention of macromolecules in the hydrogel scaffold radiolabel medium was not routinely analyzed for biosynthetic products. Peptide gel extracts were analyzed for ^{3}H-hydroxyproline content (28). The ratio of incorporated (^{3}H-hydroxyproline)/(^{3}H-proline) was multiplied by 2.2 to calculate the percent newly synthesized collagen, based on the 1:1.2 molar ratio of hydroxyproline to proline in bovine type II collagen (29). Thus, newly synthesized proteins were determined to be ≈70% collagen. These data demonstrate that the percentage of newly synthesized proteins found as collagen is similar to that observed in native calf cartilage organ cultures of the same age as the cells used in this study (30).

Histological Examination of Chondrocytes and Newly Synthesized ECM Within Peptide Hydrogels. Cell-seeded peptide specimens were fixed in 4% paraformalydehyde in PBS overnight at 4°C, washed, dehydrated with isopropanol, transferred to xylol, and embedded in paraffin. Sections 7 μm thick were made and spread on slides coated with chromealaun-gelatin (31), deparaffinated in xylol, and transferred into aqua dest by using decreasing concentrations of ethanol. Some sections were incubated for 6 min with toluidine blue dye solution [0.0714% toluidine blue (Merck), 0.0714% pyronin Y (Fluka), and borax (0.143% di-sodium-tetra-borate, Merck)],

washed subsequently with aqua dest, 96% ethanol, propanol, and xylol, and mounted on microscopic slides with DePeX (Serva).

Collagen Immunohistochemistry. Sections were treated with pepsin for 30 min, washed with TBS buffer, treated with 0.6% H_2O_2 in methanol, rinsed again with TBS, and treated with mouse anticollagen type II IgG (clone CII C1, Developmental Studies Hybridoma Bank, Iowa City, IA, 1:1,000 in TBS) for 60 min, as described (31). After incubation with rabbit anti-mouse IgG (horseradish peroxidase-conjugated Dako P-0260; 1:200 in TBS containing 1% bovine serum) for 30 min, the sections were rinsed and incubated for 30 min with goat anti-rabbit IgG (horseradish peroxidase-conjugated Dako P-0448; 1:100 in TBS containing 1% bovine serum). The samples were stained with diaminobenzidine (DAB Kit, Vector Laboratories). Cell nuclei were counterstained with Meyer's hemalum. Stained samples were embedded on microscopic slides with Aquatex (Merck).

Collagen Isolation and SDS/PAGE. Selected 3-mm cell-seeded peptide plugs (initial seeding density 15×10^6 cells per ml) cultured in ITS/FBS medium were punched on day 35 and lyophilized. Collagens were extracted with pepsin (Sigma, 1 mg/ml in 0.2 M NaCl, 0.5 M acetic acid) as described (32), except 4.5 M NaCl was used to precipitate collagen rather than ammonium sulfate. Collagens extracted from chick cartilage and mouse skin (a generous gift from P. Bruckner, University of Münster, Münster, Germany) were run in parallel to the cell-seeded peptide extract as standards for type II collagen synthesized by native chondrocytes and type I collagen synthesized by dedifferentiated fibroblastic phenotypes, respectively (P. Bruckner, personal communication).

Mechanical Properties of Cell-Seeded Hydrogels. Groups of cell-seeded peptide plugs were punched on days 0, 6, and 26 from the 10% FBS culture and day 28 of the ITS/FBS culture. The equilibrium modulus and dynamic stiffness of each plug was measured in radially confined uniaxial compression by using a Dynastat mechanical spectrometer (IMASS, Hingham, MA) as described (33). Briefly, individual specimens were placed in a confining cylindrical chamber that was clamped in the jaws of the Dynastat. A porous platen attached to the upper jaw was used to apply 4–6 sequential ramp-and-hold compressive strains of 3% to the plug (3% compression over 10 sec followed by a 1–5 min of hold), resulting in an initial increase and subsequent relaxation of the compressive stress. The ratio of the relaxed equilibrium stress to the engineering strain was used to compute the equilibrium modulus. At 18% compressive offset strain, a 1% amplitude sinusoidal strain was applied at 1.0 Hz. The dynamic compressive stiffness was calculated as the ratio of the fundamental amplitudes of stress to strain (33).

Chondrocyte Division Within Peptide Hydrogel. Peptide in digested samples was found to cause interference with the DNA spectrofluorometric measurement of Kim *et al.* (34); therefore, cell density measurements in chondrocyte-seeded peptide could not be inferred with this method. A viable cell kit based on the compound 3-(4,5-dimethylthiazol-2-yl)-5-(3-carboxymethoxyphenyl)-2-(4-sulfophenyl)-2H-tetrazolium (MTS) (Promega) was used to determine viable cell density in seeded peptide scaffolds. To establish a calibration curve for 3D cultures, five agarose slabs were seeded at cell densities ranging between 10 and 30×10^6 cells per ml. Samples were punched and analyzed on days 2, 3, and 5. For each group of 11 plugs, six were incubated in MTS medium for 2 h on a shaker table. SDS was added (final concentration = 2%) to stop the MTS reaction. The absorbance of medium samples at 490 nm was measured after 30 min. The remaining five plugs were digested and analyzed for DNA content. Mean MTS output was plotted against mean DNA content to establish the calibration curve. MTS data were then obtained for cell-seeded peptide plugs by using the established method.

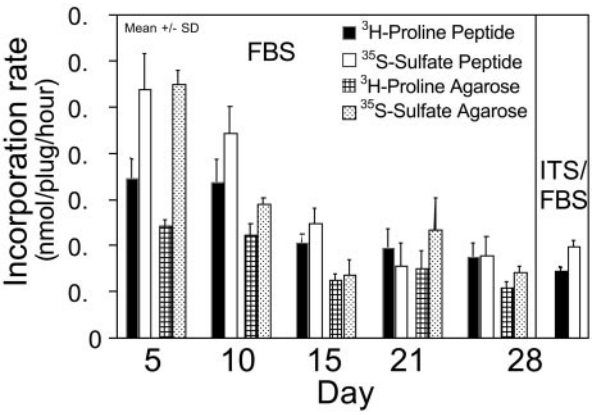

Fig. 2. Radiolabel incorporation of ^{3}H-proline and ^{35}S-sulfate as measures of the synthesis of proteins and sulfated proteoglycans, respectively, by chondrocytes within cell-seeded peptide and agarose hydrogels.

To further verify MTS results, cell-seeded peptide samples were analyzed via 5′ BrdUrd incorporation for 24 h on days 3 and 7. BrdUrd (10 μM) was added to the culture media for 24 h. Samples were fixed in 2% paraformaldehyde in PBS (pH 7.4) at room temperature, washed with PBS, and subsequently treated with 0.1% Triton X-100 in PBS for 2 h, then they were treated with 2 M HCl in PBS for 30 min at 37°C and washed with PBS. Blocking buffer (20% bovine calf serum/0.1% Triton X-100/1% DMSO in PBS) was added to the samples. An anti-BrdUrd antibody IgG_1 FITC-conjugated (PharMingen, 33284X) was used to visualize BrdUrd-positive cells under a Nikon TE 300 inverted microscope with phase contrast and fluorescence.

Results

Casting of Cell-Seeded Peptide Hydrogels. Previously, cell-free peptide hydrogels were formed by first dissolving the peptide in deionized water and then exposing the peptide solution to salt solution or culture medium to initiate self-assembly. Here, 295 mM sucrose solution was used to solubilize the KLD-12 peptide to increase osmolarity to physiological levels and thereby maintain cell viability before addition of electrolyte. Sucrose solution was found to be a suitable medium for peptide dissolution and subsequent self-assembly. Upon immersion in PBS, the casting frame produced flat slabs of chondrocyte-seeded peptide gel from which cylindrical plug samples could be cored (Fig. 1*B*). Encapsulated chondrocytes showed a round morphology within the peptide gel (Fig. 1*C*), similar to that seen in standard agarose or explant cultures. Cell viability in the peptide gel was ≈80% immediately after casting, whereas the same chondrocyte population seeded into parallel agarose culture had ≈95% viability.

Biosynthesis of ECM Macromolecules by Encapsulated Chondrocytes Within Hydrogels. Proteoglycan (^{35}S-sulfate incorporation) and protein (^{3}H-proline) synthesis rates by cells in peptide hydrogels with 10% FBS medium were initially high at early times (day 5) and then decreased by day 15 to values on the order of that in native cartilage tissue (Fig. 2) (23). Subsequent incorporation through day 28 remained relatively constant. Radioisotope incorporation in cell-seeded agarose hydrogels (Fig. 2) revealed biosynthesis levels similar to those in peptide hydrogels and comparable to values previously reported in the literature for agarose culture with bovine calf chondrocytes (23). It is important to emphasize that cell-seeded peptide plugs cultured in minimal medium (ITS/FBS) and radiolabeled on day 28 showed biosynthesis rates similar to those in agarose and peptide hydrogels with 10% FBS-supplemented rich medium.

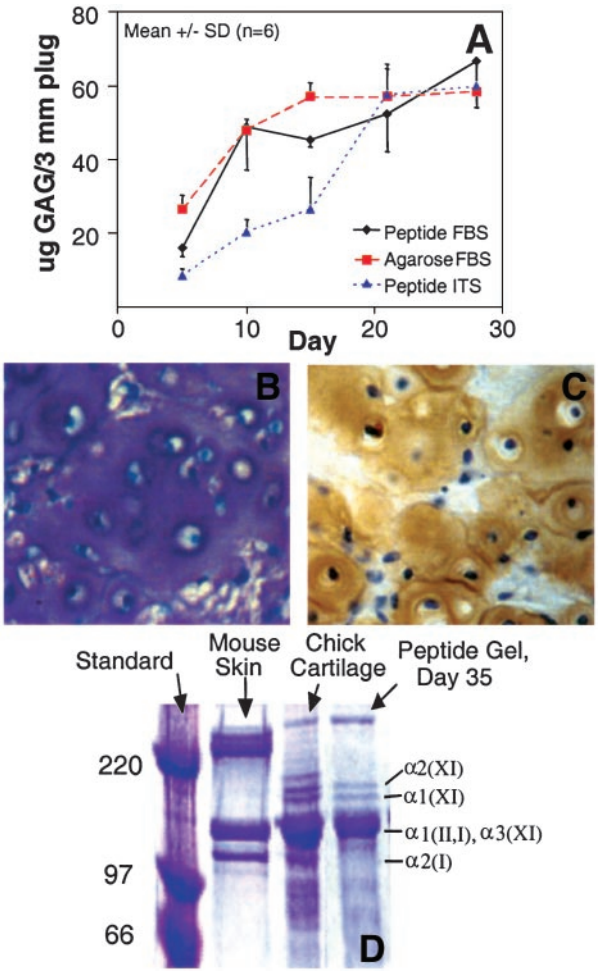

Fig. 3. Matrix accumulation in chondrocyte-seeded peptide hydrogel. (*A*) Total GAG accumulation in cell-seeded peptide hydrogel cultured in FBS and ITS/FBS medium and in cell-seeded agarose. (*B*) Toluidine blue staining of chondrocyte-seeded peptide hydrogel cultured in 10% FBS, day 15. (*C*) Immunohistochemical staining for type II collagen in cell-seeded peptide hydrogel cultured in 10% FBS, day 15. Image width for *B* and *C* = 175 μm. (*D*) SDS/PAGE of collagens extracted from day 35 samples of chondrocyte-seeded peptide hydrogel cultured in 1% ITS with 0.2% FBS. Standards: Chick cartilage for collagen II and XI banding pattern. Mouse skin identifies collagen I α-helix 2, indicative of collagen expression of a dedifferentiated, fibroblastic phenotype.

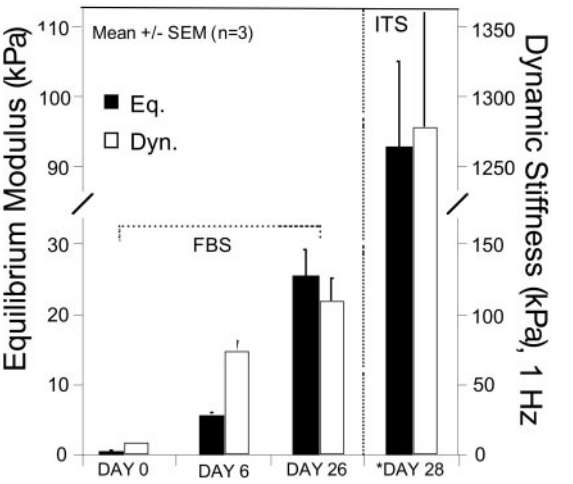

Fig. 4. Mechanical properties of chondrocyte-seeded peptide hydrogels. Equilibrium modulus and dynamic stiffness measured in uniaxial confined compression, evaluated in 6-mm diameter plugs initially seeded at a density of 15×10^6 cells per ml and cultured in 10% FBS medium. * indicates 3-mm diameter plugs seeded at 30×10^6 cells per ml and cultured in ITS/FBS medium, conditions that resulted in markedly increased stiffness values, as high as 20–33% that of human and animal cartilages (26).

GAG Accumulation Within Gel-Encapsulated ECM. Total GAG accumulation in peptide hydrogels with 10% FBS medium increased with time in culture, reaching ≈70 μg/plug by day 28 (Fig. 3*A*). Agarose cultures showed similar GAG accumulation, consistent with previous data for agarose culture (23). In ITS/FBS medium, GAG accumulation in peptide gels was initially lower than that in both agarose culture and 10% FBS peptide hydrogel cultures through day 15; however, by days 21 and 28, GAG accumulation was similar in all three cases. Toluidine blue staining of peptide hydrogels cultured in FBS medium revealed GAG accumulation throughout the peptide hydrogel matrix on day 26 (Fig. 3*B*). The majority of the chondrocytes showed a rounded morphology and were fully encapsulated within a continuous GAG-rich matrix, with a higher pericellular staining relative to the interterritorial matrix.

Chondrocyte Phenotypic Expression. Cell-seeded peptide gels cultured in FBS medium were fixed on day 15 for collagen II immunostaining. Collagen II (Fig. 3*C*) showed a staining pattern similar to that of GAG deposition, with positive staining throughout the matrix, especially in pericellular environments. Collagens from cell-seeded peptide hydrogels cultured in ITS medium were extracted on day 35 and analyzed by using SDS gel electrophoresis (Fig. 3*D*). Proteins extracted from cell-seeded peptide hydrogel showed bands for collagen type II α1 chains, as well as α1 and 2 chains for type XI collagen. No type I α 2 chains were present, as seen in skin collagen. Western analysis further confirmed electrophoresis findings. These results demonstrate unambiguously that cells seeded into peptide hydrogels maintained their chondrocyte phenotype throughout the 4-week *in vitro* culture period.

Mechanical Properties of Chondrocyte-Seeded Hydrogels. Day 0 values for equilibrium modulus were less than 1 kPa, which corresponds to the weak compressive resistance of the acellular peptide hydrogel itself (Fig. 4). Development of a continuous GAG matrix was reflected in a dramatic increase in mechanical properties over time in culture. By day 26, the equilibrium modulus increased to 26 kPa, a value about 10% of the modulus of native tissue (35). Dynamic stiffness at 1 Hz also increased with time in culture, with day 26 values about 5% of those of native tissue (35). Interestingly, cells seeded into peptide hydrogels at 30×10^6 cells per ml and cultured in ITS/FBS medium showed an even more profound increase in compressive stiffness. The equilibrium modulus reached 93 kPa by day 28, and the dynamic stiffness at 1 Hz reached 1.28 MPa (Fig. 4), both values being ≈1/5 to 1/3 that of native human and animal articular cartilages (36).

Encapsulated Cell Division. Calibration of the MTS viable cell assay in cell-seeded agarose plugs showed linear behavior over a range of cell densities (Fig. 5*A*). Cell-seeded peptide hydrogels and agarose gels cultured in FBS medium were evaluated for viable cell density by using the MTS assay (Fig. 5*B*). In agarose gels, viable cell density increased by 20% between day 2 and day 7 of culture, an increase similar to that previously reported with DNA (Hoechst dye) analysis (23). In contrast, peptide hydrogels showed a more dramatic 80% increase in viable cell density between days 2 and 9 of culture. BrdUrd incorporation in cell-seeded peptide hydrogels further delineated MTS results (Fig. 5 *C* and *D*). A significant fraction of cells within the peptide hydrogel labeled positively for BrdUrd incorporation during the 24-h incubation period on days 2–3 and 7–8, further indicating a significant content of dividing cells in these cultures.

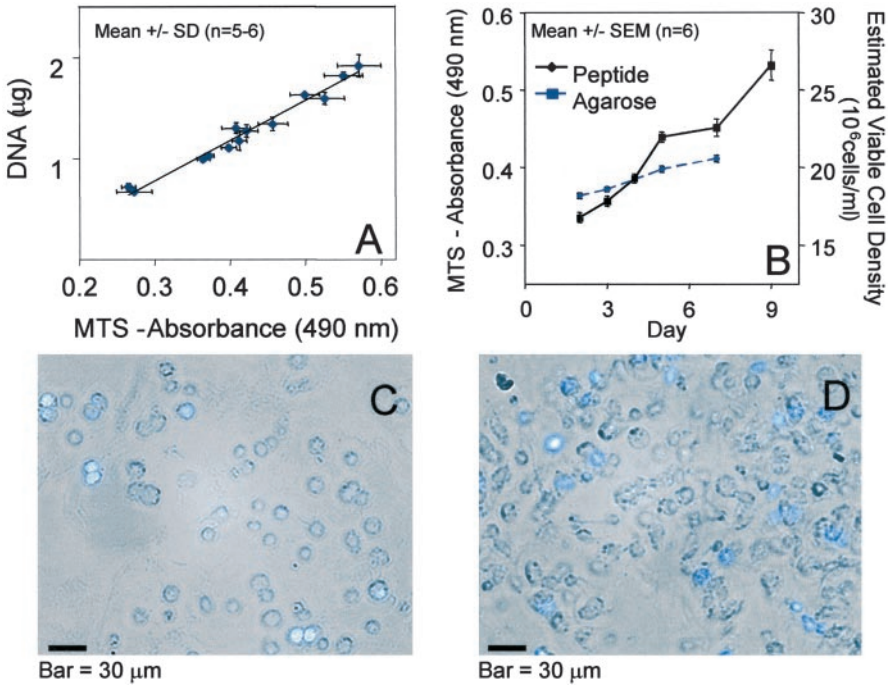

Fig. 5. Cell division of chondrocytes seeded in peptide hydrogel. (*A*) Calibration curve for the MTS assay in chondrocyte-seeded agarose hydrogel. (*B*) MTS measurement of the density of cells in chondrocyte-seeded peptide and agarose hydrogels. (*C* and *D*) BrdUrd incorporation in chondrocyte-seeded hydrogel 3 days (*C*) and 7 days (*D*) after seeding.

Discussion

Casting of Cell-Seeded Peptide Hydrogels. The casting procedures developed here enabled rapid and efficient encapsulation of chondrocytes within peptide hydrogels while maintaining high cell viability (>80%). Encapsulated cells were evenly distributed throughout the hydrogel. In this study, cell-seeded hydrogels were cast in a flat slab geometry to enable quantification of biomechanical properties and normalization of ECM biosynthesis and accumulation to a constant plug volume. However, this casting technique is generally applicable for scaffolds of arbitrary geometry and other cell types, a very important feature for applications in tissue repair. Here, peptides self-assemble into well-ordered nanofibers with inter-fiber spaces ≈50–200 nm and, simultaneously, into a nanoscale hydrogel network (15–17) around each individual chondrocyte in the cell-peptide solution. This intimate cell-scaffold architecture may offer unique advantages regarding peptide-cell signaling and cell-mediated peptide biodegradability.

Chondrocyte Appearance and Division Within the Peptide Hydrogel. Chondrocyte-seeded constructs for cartilage repair may benefit from cell division after seeding in the scaffold to further increase the number of ECM-producing cells. The peptide hydrogel matrix appeared favorable for cell division while maintaining synthesis of phenotypically specific ECM macromolecules. Division of encapsulated chondrocytes was substantially higher in peptide gels relative to agarose control cultures. Abundant cell pairs undergoing cell division were observed within the hydrogel as early as day 3 in culture (Fig. 5 *B–D*). It is not known whether higher cell division in peptide hydrogel relative to agarose can be attributed to cell-peptide interactions, physical environment, or other factors. Ongoing studies exploring specific cell-peptide interactions may give insights into methods for further stimulation of cell division.

Synthesis and Accumulation of ECM Within Peptide Hydrogels. Radiolabel incorporation and total GAG accumulation (Figs. 2 and 3*A*) were normalized on a per-plug basis, as punched from parent slab gels. In this manner, biosynthesis is reported as representative repair tissue generation for a given initial scaffold geometry (e.g., a cylindrical disk specimen) and cell-seeding density. Radiolabel incorporation (Fig. 2) showed that synthesis of proteoglycans and total protein by primary calf chondrocytes was similar in 3D agarose and 3D peptide hydrogel culture. Thus, specific differences in hydrogel composition and microphysical environment between peptide and agarose scaffolds did not significantly affect the net rates of cell synthesis of ECM macromolecules.

Total GAG accumulation in cell-seeded peptide scaffold was also similar to that in agarose culture (Fig. 3*A*), despite the differences in scaffold concentration (0.5% vs. 2% wt/wt). For comparison with other studies in the literature, data from day 15 (Fig. 3*A*) were normalized to DNA content 7.7 pg DNA/cell (34) based on an estimate of the cell density at day 15 (assumed to be ≈2× the initial seeding density from the trends of Fig. 5*B*). Thus, the computed GAG density on day 15 was ≈22 μg/μg DNA. This value is less than that reported in alginate culture (≈50 μg/μg) (25) but greater than that in type I collagen sponge (4.8 μg/μg) (37), polyglycolic acid (≈8 μg/μg) and polylactic acid (≈5 μg/μg) (6). In addition, the percent GAG normalized to wet weight in peptide scaffold (estimate ≈0.9%, week 4) compared with polyethylene oxide, ≈0.23%, week 6, 50×10^6 cells per ml initial seeding density (9). Although direct comparisons are difficult because of inconsistent factors such as seeding density and culture medium, GAG accumulation in our peptide hydrogel scaffold appears to be within the range of other polymer and hydrogel scaffolds.

The majority of our experiments used a seeding density of 15×10^6 cells per ml in culture with 10% FBS. Such conditions are convenient for comparison to previously published studies but are not necessarily optimal for *in vitro* development of repair tissue. Limited studies using different medium and cell densities were also conducted to demonstrate options for *in vitro* culture conditions. ITS-based, low serum medium (0.2% FBS) was found to be comparable to 10% FBS + DMEM in terms of total GAG accumulation and radioisotope incorporation (on day 28, Fig. 2). However, a 2-fold increase in cell seeding density in combination with culture in ITS/FBS medium resulted in a 4-fold increase in equilibrium compressive modulus and >10-fold increase in dynamic stiffness, much more than would be expected from a proportional increase in seeding density alone. Such variables therefore should be explored in detail to further optimize a chondrocyte/peptide-hydrogel system for clinical use in cartilage repair.

Biomechanical Properties. GAG accumulation in seeded peptide scaffold was distributed throughout the hydrogel, in both cell-

associated and interterritorial space (Fig. 3*B*). The development of continuous ECM was reflected in the increase in compressive stiffness as a function of time in culture (Fig. 4). On day 0 the peptide hydrogel-seeded with 15×10^6 cells per ml was very fragile, with extremely low compressive stiffness (100–1,000 times lower than native cartilage). After 6 days in culture, the handling properties of the plugs were noticeably improved, with equilibrium modulus increasing by almost an order of magnitude. By day 26 the test samples could be freely handled and attained an equilibrium modulus of 26 kPa (approximately 30-fold increase compared with day 0). For comparison, the equilibrium modulus of polyglycolic acid scaffolds seeded with primary calf chondrocytes at $\approx 125 \times 10^6$ cells per ml and cultured in free-swelling conditions was ≈52 kPa after 42 days (38), and the modulus of peptide hydrogel scaffolds with 30×10^6 cells per ml in ITS/FBS was 93 kPa (Fig. 4).

Immunohistochemical analysis for type II collagen showed positive staining throughout the peptide hydrogel in a continuous manner, whereas type I collagen staining appeared at only background levels around cells within the gel. With 10% FBS-supplemented medium, positive type I collagen staining was observed within a thin layer of fibroblastic-like cells that showed increasing cell numbers with time in culture only on the outer surfaces of the gel. Interestingly, cell-seeded peptide hydrogels cultured in ITS/FBS medium were observed to have much less dedifferentiation and fibroblast-like cell accumulation on the surface. Therefore, cell samples were chosen from ITS/FBS culture for collagen content analysis. SDS-gel electrophoresis confirmed accumulation of predominantly type II collagen in the cell-seeded peptide hydrogel culture (Fig. 3*D*).

An Emerging Biomaterial for Regenerative Medicine. Our study demonstrates the potential of a self-assembling peptide scaffold to maintain differentiated chondrocytes and stimulate the synthesis and accumulation of a mechanically functional cartilage-like ECM in a 3D cell culture. The peptide KLD12 used in this study represents one of a class of specially designed self-assembling peptides developed through molecular engineering. The synthetic nature of the material allows for single amino acid design, with sequences tailored for cell signaling and/or scaffold degradation. Self-assembly of this class of peptides occurs at physiological electrolyte concentrations and pH, without toxic processing procedures. However, each peptide must first be carefully screened *in vivo* to ensure the sequence does not elicit an immunogenic response by the host animal.

The optimal peptide hydrogel scaffold for successful cartilage tissue repair must enable long-term tissue formation and integration with surrounding tissue *in vivo*. Our ongoing studies are aimed at optimization of cartilage ECM development within the peptide for *in vivo* implantation. ECM synthesis may be further stimulated by addition of growth factors (39) and culture in bioreactors that increase nutrient transport (5, 37, 38) and apply mechanical loads (40, 41). The interaction between chondrocyte and peptide matrix is being investigated by designing binding sites in the peptide sequence. Furthermore, peptides can be designed to include specific sites to enable enzymatic degradation by matrix metalloproteinases and aggrecanases that are naturally synthesized by chondrocytes. In this manner, spatial and temporal control of scaffold biodegradability may be obtained. In addition, the synthetic manufacturing of peptides may allow for tethering of growth factors to subpopulations of peptide units, enabling controlled concentrations of growth factors to be directly delivered to encapsulated cells. Such flexibility offers a broad spectrum of opportunities to investigate multiple approaches toward generating the appropriate tissue repair response. Finally, previous studies have shown that dynamic mechanical compression (27) and shear (42) loading of cartilage explants can dramatically stimulate proteoglycan and collagen synthesis relative to unloaded control cultures. Therefore, mechanical loading of self-assembling peptide gel-encapsulated chondrocytes may stimulate development of an ECM that is rich in proteins or proteoglycans relative to standard free-swelling culture. Such strategies may be useful in developing unique ECM components in cell-seeded peptide scaffolds for repairing cartilage defects in the body.

We thank Michael Caplan, Alex Schermer, and Tom Crowell for their technical consultation. This work was supported in part by grants from the National Institutes of Health (Grant AR33236) and the DuPont–Massachusetts Institute of Technology Alliance.

1. Brittberg, M., Lindahl, A., Nilsson, A., Ohlsson, C., Isaksson, O. & Peterson, L. (1994) *N. Engl. J. Med.* **331,** 889–895.
2. Glowacki, J. (2000) *J. Rehabil. Res. Dev.* **37,** 171–177.
3. Schuman, L., Buma, P., Versleyen, D., de Man, B., van der Kraan, P. M., van den Berg, W. B. & Homminga, G. N. (1995) *Biomaterials* **16,** 809–814.
4. Nehrer, S., Breinan, H. A., Ramappa, A., Shortkroff, S., Young, G., Minas, T., Sledge, C. B., Yannas, I. V. & Spector, M. (1997) *J. Biomed. Mater. Res.* **38,** 95–104.
5. Grande, D. A., Halberstadt, C., Naughton, G., Schwartz, R. & Manji, R. (1997) *J. Biomed. Mater. Res.* **34,** 211–220.
6. Freed, L. E., Marquis, J. C., Nohria, A., Emmanual, J., Mikos, A. G. & Langer, R. (1993) *J. Biomed. Mater. Res.* **27,** 11–23.
7. Perka, C., Spitzer, R. S., Lindenhayn, K., Sittinger, M. & Schultz, O. (2000) *J. Biomed. Mater. Res.* **49,** 305–311.
8. Hauselmann, H. J., Fernandes, R. J., Mok, S. S., Schmid, T. M., Block, J. A., Aydelotte, M. B., Kuettner, K. E. & Thonar, E. J. (1994) *J. Cell Sci.* **107,** 17–27.
9. Bryant, S. J. & Anseth, K. S. (2001) *Biomaterials* **22,** 619–626.
10. Wakitani, S., Goto, T., Young, R. G., Mansour, J. M., Goldberg, V. M. & Caplan, A. I. (1998) *Tissue Eng.* **4,** 429–444.
11. Nehrer, S., Breinan, H. A., Ramappa, A., Hsu, H. P., Minas, T., Shortkroff, S., Sledge, C. B., Yannas, I. V. & Spector, M. (1998) *Biomaterials* **19,** 2313–2328.
12. Fragonas, E., Valente, M., Pozzi-Mucelli, M., Toffanin, R., Rizzo, R., Silvestri, F. & Vittur, F. (2000) *Biomaterials* **21,** 795–801.
13. Elisseeff, J., Anseth, K., Sims, D., McIntosh, W., Randolph, M. & Langer, R. (1999) *Proc. Natl. Acad. Sci. USA* **96,** 3104–3107.
14. Grigolo, B., Roseti, L., Fiorini, M., Fini, M., Giavaresi, G., Aldini, N. N., Giardino, R. & Facchini A. (2001) *Biomaterials* **22,** 2417–2424.
15. Zhang, S., Holmes, T., Lockshin, C. & Rich, A. (1993) *Proc. Natl. Acad. Sci. USA* **90,** 3334–3338.
16. Zhang, S., Holmes, T. C., DiPersio, C. M., Hynes, R. O., Su, X. & Rich, A. (1995) *Biomaterials* **16,** 1385–1393.
17. Holmes, T. C., de Lacalle, S., Su, X., Liu, G., Rich, A. & Zhang, S. (2000) *Proc. Natl. Acad. Sci. USA* **97,** 6728–6833.
18. Caplan, M. R., Moore, P. N., Zhang, S., Kamm, R. D. & Lauffenburger, D. A. (2000) *Biomacromolecules* **1,** 627–631.
19. Marini, D. M., Hwang, W., Lauffenburger, D. A., Zhang, S. & Kamm, R. D. (2002) *Nanoletters* **2,** 295–259.
20. Holmes, T. C. (2002) *Trends Biotechnol.* **20,** 16–21.
21. Benya, P. D. & Shaffer, J. D. (1982) *Cell* **30,** 215–224.
22. Lemare, F., Steimberg, N., Le Griel, C., Demignot, S. & Adolphe, M. (1998) *J. Cell. Physiol.* **176,** 303–313.
23. Buschmann, M. D., Gluzband, Y. A., Grodzinsky, A. J., Kimura, J. H. & Hunziker, E. B. (1992) *J. Orthop. Res.* **10,** 745–758.
24. Buschmann, M. D., Gluzband, Y. A., Grodzinsky, A. J. & Hunziker, E. B. (1995) *J. Cell Sci.* **108,** 1497–1508.
25. Ragan, P. M., Chin, V. I., Hung, H. H., Masuda, K., Thonar, E. J., Arner, E. C., Grodzinsky, A. J. & Sandy, J. D. (2000) *Arch. Biochem. Biophys.* **383,** 256–264.
26. Hascall, V. C., Handley, C. J., McQuillan, D. J., Hascall, G. K., Robinson, H. C. & Lowther, D. A. (1983) *Arch. Biochem. Biophys.* **224,** 206–223.
27. Sah, R. L., Kim, Y. J., Doong, J. Y., Grodzinsky, A. J., Plaas, A. H. & Sandy, J. D. (1989) *J. Orthop. Res.* **7,** 619–623.
28. Stern, B. D., Mechanic, G. L. & Glimcher, M. J. (1963) *Biochem. Biophys. Res. Commun.* **13,** 137–143.
29. Herbage, D., Bouillet, J. & Bernengo, J.-C. (1977) *Biochem. J.* **161,** 303–312.
30. Sah, R. L., Doong, J. Y., Grodzinsky, A. J., Plass, A. H. K. & Sandy, J. D. (1991) *Arch. Biochem. Biophys.* **286,** 20–29.
31. Domm, C., Schünke, M., Christesen, K. & Kurz, B. (2002) *Osteoarthritis Cart.* **10,** 13–22.
32. Bruckner, P., Horler, I., Mendler, M., Houze, Y., Winterhalter, K. H., Eich-Bender, S. F. & Spycher, M. A. (1989) *J. Cell Biol.* **109,** 2537–2545.
33. Frank, E. H. & Grodzinsky, A. J. (1987) *J. Biomech.* **20,** 615–627.
34. Kim, Y. J., Sah, R. L., Doong, J. Y. & Grodzinsky, A. J. (1988) *Anal. Biochem.* **174,** 168–176.
35. Eisenberg, S. R. & Grodzinsky, A. J. (1985) *J. Orthop. Res.* **3,** 148–159.
36. Chen, A. C., Bae, W. C., Schinagl, R. M. & Sah, R. L. (2001) *J. Biomech.* **34,** 1–12.
37. Mizuno, S., Allemann, F. & Glowacki, J. (2001) *J. Biomed. Mater. Res.* **56,** 368–375.
38. Vunjak-Novakovic, G., Martin, I., Obradovic, B., Treppo, S., Grodzinsky, A. J., Langer, R. & Freed, L. E. (1999) *J. Orthop. Res.* **17,** 130–138.
39. van Osch, G. J., van den Berg, W. B., Hunziker, E. B. & Hauselmann, H. J. (1998) *Osteoarthritis Cart.* **6,** 187–195.
40. Frank, E. H., Jin, M., Loening, A. M., Levenston, M. E. & Grodzinsky, A. J. (2000) *J. Biomech.* **33,** 1523–1527.
41. Mauck, R. L., Soltz, M. A., Wang, C. C., Wong, D. D., Chao, P. H., Valhmu, W. B., Hung, C. T. & Ateshian, G. A. (2000) *J. Biomech. Eng.* **122,** 252–260.
42. Jin, M., Frank, E. H., Quinn, T., Hunziker, E. B. & Grodzinsky, A. J. (2001) *Arch. Biochem. Biophys.* **395,** 41–48.